SCIENCE CHINA
Information Sciences

• RESEARCH PAPERS •

December 2010 Vol. 53 No. 12: 2664–2674
doi: 10.1007/s11432-010-4110-x

The impact of time synchronization error on passive coherent pulsed radar system

HE You[1], ZHANG CaiSheng[1,2]*, DING JiaHui[2] & TANG XiaoMing[1]

[1]*Research Institute of Information Fusion, Naval Aeronautical and Astronautical University, Yantai* 264001*, China;*
[2]*Nanjing Research Institute of Electronics Technology, Nanjing* 210039*, China*

Received May 18, 2010; accepted August 9, 2010

Abstract Passive bistatic coherent radar system operates with distinct non-cooperative transmitter and receiver located at different sites. In such spatial separation, the receiving system needs to independently solve the problem of time and phase synchronization via direct-path signal. The impact of time synchronization error was explored and solved in passive bistatic coherent radar. The common model of digital sampling process is introduced to illustrate the effect of time synchronization error (TSE). The periodicity of relative sample instant variation of each pulse is deduced. Then, normalized interference power (NIP) is defined to evaluate the potential impact of TSE. The NIP expressions are derived when the difference between the adjacent relative sample instant is uniform distribution or Gaussian distribution. It is found that there are new spurious frequency components and the detection performance is decreased in the case of asynchronous sampling. At the same time, the analytical Doppler frequency bias expression caused by TSE is presented. Theoretical results are confirmed by simulation in the cases of different periods of relative sampling instant.

Keywords passive coherent radar (PCR), time synchronization error (TSE), normalized interference power (NIP)

Citation He Y, Zhang C S, Ding J H, et al. The impact of time synchronization error on passive coherent pulsed radar system. Sci China Inf Sci, 2010, 53: 2664–2674, doi: 10.1007/s11432-010-4110-x

1 Introduction

One premise of digital coherent signal processing for Doppler radar is keeping the coherence between pulses after data sampling. Several restrictions on digital sampling parameters are proposed in [1, 2]. In order to guarantee the coherence between pulses, the sampling clock and trigger signal must synchronize to the pulse repetition frequency (PRF) of non-cooperative transmitting signal. The performance of time synchronization will directly affect the coherent signal processing gain [3].

One of the most critical issues for coherent detection in passive coherent pulsed radar is time synchronization. The only technique of time synchronization for passive coherent pulsed radar, however, is to synchronize the sampling clock by direct-path signal in the passive receiving system [4–7]. In practice, even if the direct-path signal can be received successively during the scanning of the transmitter's antenna, the signal-to-noise ratio of direct-path signal will affect the accuracy of PRF estimation. As a

*Corresponding author (email: caifbi2008@yahoo.com.cn)

result, there is TSE between the time-base of sampling clock and target echo. The number of samples per PRF may be not an integer, and the relative sample instant will drift, too. In the process of digital signal processing, however, the independent variable in the sampling sequence has no information about the jitter of timing clock.

Jenq [8, 9] first described and analyzed the spectrum of ideal sine wave in the case of non-uniformly sampling. Its original idea is decomposing the non-uniformly sampled sequence into M subsequences, which are subsequently treated as uniformly sampled data. The digital spectral representation of a non-uniformly sampled sequence data is proposed in terms of its analog spectrum. Based on this research, ref. [10] explored a more generalized digital spectral expression for non-uniformly sampled signal. Perfect reconstruction algorithm of digital spectrum from non-uniformly sampled signals is proposed if timing error in the receiving system is known [11]. Some special cases on the spectrum reconstruction algorithm are presented in [3, 12].

In this paper, we concentrate on the impact of TSE on coherent detection and Doppler shift estimation in passive coherent pulsed radar system. The common model of digital sampling process is described in section 2. The period of relative sample instant variation of each pulse is explored via modeling in section 3. In section 4, NIP is defined to assess the potential impact of the TSE on coherent detection and Doppler shift estimation. The NIP expressions are derived when the difference between the adjacent relative sample instant is uniform distribution or Gaussian distribution. Finally, conclusions are presented in section 5.

2 Problem description

A scenario with non-cooperative radar illuminator considered in this paper is illustrated in Figure 1. Assume that the transmitter is mechanically scanned in azimuth, and the receiver is stationary while the target is moving. Both the transmitter and receiver are focusing on the moving target. The receiving system intercepts the direct-path waveform transmission through a reference antenna when it tunes to the transmitting frequency, and target reflection echoes are intercepted by the target antenna. Time and phase synchronization need to be completed via direct-path signal. Then, optimum detection and parameters estimation are commonly involved in passive coherent processing. Surveillance and early-warning may be achieved in the area of interest [13, 14].

According to the Nyquist sampling theorem, the sampling frequency F_s must not be less than $2F_c$, where F_c is the carrier frequency of transmitting signal. In practice, however, in coherent pulse radar, the coherence is required among pulses after data sampling process. Generally speaking, the common sampling process can be described as Figure 2. For convenience, the rising edge of each pulse is defined as the starting instant of the corresponding PRF. Here, δt_i denotes the interval between the first sample instant of the ith pulse, and $0 \leqslant \delta t_i \leqslant T_s$, where T_s is sampling interval. Then, δt_1 is fixed time delay between the sampling clock and the rising edge of the first pulse caused by signal transmission. For the purpose of coherent processing, it is desired that $\delta t_1 = \delta t_2 = \cdots = \delta t_i$. In this way, we should guarantee that $F_s = pf_r$, $p = 1, 2, 3, \ldots$, where f_r is the value of PRF.

In the passive coherent radar system, however, we need to estimate the PRF of the transmitting signal via direct-path pulses. In theory, the direct-path signal is modulated by the rotating transmitter's antenna pattern, which will reduce the estimation accuracy of PRF, and hence TSE between the sample frequency and PRF is introduced unconsciously.

Assume that the range sweep is initiated by a threshold detection of the direct-path pulse. In a passive bistatic receiving system, we designate the first sample of each direct-path pulse crossed the threshold as the trigger of sampling clock. There is a series of data samples in every pulse repetition interval (PRI). With no loss of generality, the sampling process of target reflection echoes in the target dwell time can be illustrated as Figure 3. It can be found that the first sample instant of each pulse is drifting relative to the start of the direct pulse. Note that sample 1 is the first sample of direct-path pulse from PRI 1 to PRI 4. However, sample 4 will be the first sample of direct-path pulse from PRI 5 to PRI 8 and the process will be repeated. For the case of a general direct path pulse shape, the net result of this asynch-

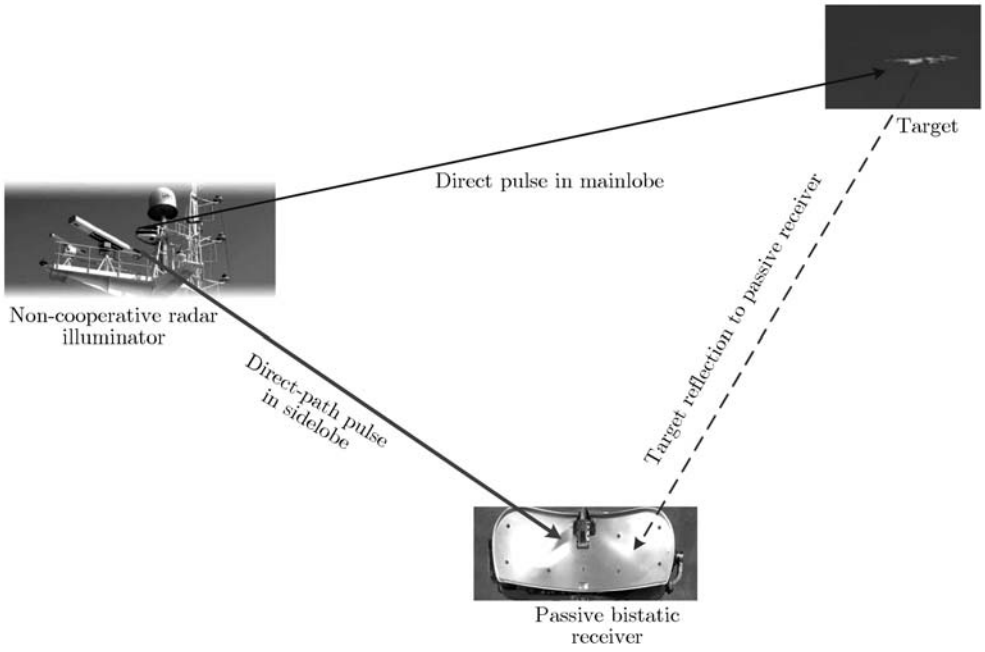

Figure 1 Signal paths in passive coherent pulsed radar system.

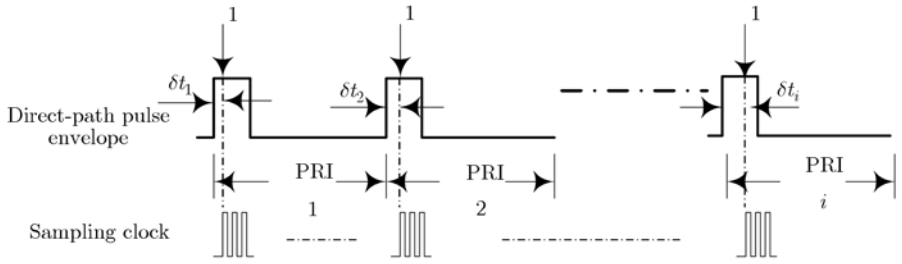

Figure 2 Sketch map of coherent pulses sampling.

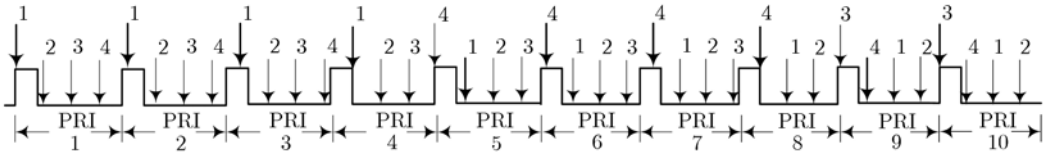

Figure 3 Sketch map of relative sample instances change.

ronous sampling is an unintentional periodicity in the data. In this simple case, the period of the variation is 4 PRIs. Another way to analysis this sample process is to recognize that there is no constant number of samples per PRI. In this case, there is a constant number of samples per PRI up to the 4th PRI, which has one less sample than the other three. In fact, there is one less sample per PRI every 4 PRIs. Then, the asynchronous sampling will cause unintentional periodicity of data sample per PRI. If the first 5 pulse samples were adopted for coherent integration, it is obvious that the first sample of the 5th pulse has no contribution for this integration. Therefore, the available pulses for coherent integration is reduced if the sampled signal cannot be reconstructed coherently. In the spectrum analysis of any range gate in direct-path channel or target reflection channel, it is speculated that there are spurious spectra caused by the unintentional data sampling periodicity.

3 Periodicity of relative sampling instant

Let the PRI of the transmitted waveform be T_r and the sampling frequency be $F_s = 1/T_s$, where T_s is sampling interval. The number of data samples per PRI is $N_p = T_r/T_s$. N_p is not an integer, in general.

If the first sampling instant of the first pulse is δt_1, then the first sampling instant of the second pulse is $[\text{int}(N_p+1)]T_s+\delta t_1$, where $\text{int}(x)$ returns the integer part of the argument. Similarly, if $(n-1)N_p$ is an integer, then the first sampling instant of the nth pulse $t(n,i)$ is $[(n-1)N_p+1]T_s+\delta t_1$; otherwise $\text{int}[(n-1)N_p+1]T_s+\delta t_1$, i.e.

$$t(n,1)=\begin{cases}[(n-1)N_p+1]T_s+\delta t_1, & \text{for } [(n-1)N_p+1]T_s \text{ is integer},\\ \text{int}[(n-1)N_p+1]T_s+\delta t_1, & \text{otherwise.}\end{cases} \tag{1}$$

Similarly, the ith sampling instant of the nth pulse is

$$t(n,i)=\begin{cases}[(n-1)N_p+(i-1)]T_s+\delta t_i, & \text{for } [(n-1)N_p+(i-1)]T_s \text{ is integer},\\ \text{int}[(n-1)N_p+(i-1)]T_s+\delta t_i, & \text{otherwise.}\end{cases} \tag{2}$$

In order to evaluate the relative periodicity of sampling instant, we should determine the first sampling instant δt_n with respect to the beginning of each pulse. This can be determined by Figure 3, i.e.

$$\delta t_n=\text{mod}(\text{mod}(\text{int}[(n-1)N_p+1]T_s+\delta t_1,T_r),T_s), \tag{3}$$

where $\text{mod}(a,b)$ returns the modulo of a with respect to b. For convenience, the constant time delay caused by the system is neglected. If $\delta t_1=0$, then the first sampling instant of the second pulse is $4T_s$. In practice, however, the first sampling instant of the 2nd pulse is $N_p=3.75$ since N_p is not an integer. And then $\delta t_2=3.75T_s$. From eq. (3) for $n=2$, we have

$$\delta t_2=\text{mod}(\text{mod}(\text{int}[3.75+1]T_s+\delta t_1,3.75T_s),T_s)=0.25T_s. \tag{4}$$

Similarly, we can get $\delta t_3=0.5T_s$, $\delta t_4=0.75T_s$, $\delta t_5=0.0$, $\delta t_6=0.25T_s$, which are corresponding to sampling instants $0.0T_s$, $0.25T_s$, $0.5T_s$, $0.75T_s$, $0.0T_s$, $0.25T_s,\ldots$. And the periodicity in this case is 4 PRIs (see Figure 3).

In general, the periodicity of relative sampling instant is equal to $PRI/\overline{frac}(N_p)$, and $\overline{frac}(N_p)$ is defined as

$$\overline{frac}(N_p)=\begin{cases}frac(N_p), & \text{for } 0<frac(N_p)<0.5,\\ 1-frac(N_p), & \text{for } 0.5<frac(N_p)<1,\end{cases} \tag{5}$$

where $frac(.)$ returns the fractional part of the argument.

In fact, let the minimum periodicity of relative sampling instant δt_i be MT_r, and the total number of data samples in M PRIs be L, i.e. $MT_r=LT_s$, where M and L are minimum integers satisfying this equation. Then

$$L=MN_p=M(\text{int}(N_p)+Mfrac(N_p)). \tag{6}$$

Obviously, $M\text{int}(N_p)$ is an integer, then it is required that

$$frac(N_p)M=n,\quad n=1,2,3,\ldots. \tag{7}$$

Generally, if $\text{mod}(1,\overline{frac}(N_p))=0$, then

$$M=1/\overline{frac}(N_p). \tag{8}$$

For example, if $N_p=10.5$, then the periodicity of asynchronous sampling will be 2 PRIs, and the number of samples per PRI varies by 1 every other PRI, i.e. 10,11,10,11, ...; and if $N_p=10.2$, then the periodicity will be 5 PRIs, etc. Another way to look at this phenomenon is to recognize that there is one more sample every M PRIs if $\overline{frac}(N_p)<0.5$, and one less sample every M PRIs for $\overline{frac}(N_p)>0.5$. In some particular cases, if $\text{mod}(1,\overline{frac}(N_p))\neq 0$, the periodicity of asynchronous sampling cannot be expressed in integer times of PRI. For instance, if $\overline{frac}(N_p)=0.3$, the periodicity would be 3.33 PRIs, approximately. Then, we may reexpress the periodicity by sampling interval.

4 Impact of TSE on coherent detection and Doppler shift estimation

Let $N = kM+N$, where $N = 0, 1, 2, 3, \ldots$, $k = 0, 1, 2, 3, \ldots$, $n = 0, 1, 2, \ldots, M-1$. Then the ith sampling instant of the Nth pulse will be

$$t(N,i) = \begin{cases} [(n-1)N_p + (i-1)]T_s + kMT_r + \delta t_1, & \text{for } (n-1)N_p \text{ is integer,} \\ \text{int}[(n-1)N_p + (i-1)]T_s + kMT_r + \delta t_1, & \text{otherwise.} \end{cases} \tag{9}$$

Denote $t(N,i)$ by δt_n, then

$$t(N,i) = kMT_r + (n-1)T_r + \delta t_n + (i-1)T_s. \tag{10}$$

With no loss of generality, let the ith data sample of the nth in-phase and quadrature digital samples in the target channel be

$$e_{\text{IF}}(N,i) = A_s \widetilde{S}_T(t(N,i)) \exp[2\pi(F_{\text{IF}} + f_d)(kMT_r + (n-1)T_r + \delta t_n + (i-1)T_s)], \tag{11}$$

where A_s is fading factor of amplitude in target-path channel, F_{IF} is intermediate frequency, $\widetilde{S}_T(t)$ is complex envelope of the transmitted waveform, f_d is bistatic Doppler shift of target, and $1 \leqslant i \leqslant T/T_s$. We will neglect the noise terms since the focus of this paper is the impact of TSE. Similarly, assume that the ith data sample of the Nth in-phase and quadrature digital samples in the direct-path channel be

$$d_{\text{IF}}(N,i) = A_d \widetilde{S}_T(t(N,i) + \tau) \exp[2\pi F_{\text{IF}}(kMT_r + (n-1)T_r + \delta t_n + (i-1)T_s + \tau)], \tag{12}$$

where A_d is fading factor of amplitude in direct-path channel, and τ is time delay of target-path channel with respect to the direct-path channel, $0 < \tau < T_r$.

According to [15–17], both detection and joint estimation of time delay and Doppler shift of target are based on the cross-ambiguity function (CAF) between direct-path signals and target echoes, in passive bistatic radar system. Its discrete form can be expressed as (see [17])

$$|\Psi(\tau, f_d)| = \left| \sum_{n=0}^{N-1} e(n) d^*(n-\tau) \exp\left(\text{j}\frac{2\pi f_d n}{N}\right) \right|. \tag{13}$$

The most obvious way to implement this processing would be to calculate the discrete Fourier transform (DFT) of $e(n)d^*(n-\tau)$ for each range bin of interest. If the time delay and Doppler shift are compensated appropriately, then the product of $e(n)d^*(n-\tau)$ can be expressed as

$$x(N,i) = A_d A_s \widetilde{S}_T^2(t(N,i)) \exp\{\text{j}2\pi f_d(kMT_r + (n-1)T_r + \delta t_n + (i-1)T_s)\}. \tag{14}$$

To get rid of the effect of the fluctuating amplitude of direct-path signal, it is necessary to normalize eq. (14) by the direct-path signal's amplitude. Thus, we have

$$\widetilde{x}(N,i) = A_s \widetilde{S}_T(t(N,i)) \exp\{\text{j}2\pi f_d(kMT_r + (n-1)T_r + \delta t_n + (i-1)T_s)\}. \tag{15}$$

In general, during the process of passive coherent processing, we take it for granted that data sampling is synchronous. If we take the ith sample of N pluses for integration, then

$$X(f,i) = \frac{A_s}{T_r} \sum_{l=-\infty}^{+\infty} A(l) S(f - f_d - l f_r/M) \exp\left(-\text{j}2\pi \frac{liT_s}{MT_r} \right), \tag{16}$$

where $A(l) = \sum_{n=0}^{M-1} 1/M \exp(\text{j}2\pi f_d \delta t_n) \exp(-\text{j}2\pi ln/M))$, $S(f) = \text{FT}[\widetilde{S}_T(t)]$. The detailed derivation of eq. (16) is given in Appendix.

In theory, $A(l)$ can be treated as the DFT of the sequence $1/M \exp(\text{j}2\pi f_d \delta t_n) \exp(-\text{j}2\pi ln/M)$, and its periodicity is M, and the periodicity of $X(f,i)$ is f_r. Furthermore, one period of the spectrum comprises M line spectra, with neighboring spectral lines separated by the amount of f_r/M. $X(f,i)$ is uniformly

spaced on the frequency axis. The Doppler shift component is located at f_d with magnitude $|A(0)|$, while the lth spectral line is located at $f_d + lf_r/M$ with magnitude $|A(l)|$. All these spurious spectral lines are located in the vicinity of Doppler shift component f_d, which may cause false alarm in these cells. Thus, we take these spectral lines as interferences. The larger the M is, the more interferences will arise.

By the theorem of Parseval, we can get

$$\sum_{n=0}^{M-1} \left| \frac{1}{M} \exp(\mathrm{j}2\pi f_d \delta t_n) \right|^2 = \frac{1}{M} \sum_{l=0}^{M-1} |A(l)|^2. \tag{17}$$

Then $\sum_{l=0}^{M-1} |A(l)|^2 = 1$, meaning that asynchronous sampling gives rise to energy leakage to the spectral lines of $f_d + lf_r/M$.

While in the synchronization case, i.e. $\delta t_n = 0$, $A(l) = \begin{cases} 1, & \text{for } l = 0, M, 2M, \dots \\ 0, & \text{otherwise} \end{cases}$, and the neighboring spectral lines are separated by the amount of f_r, which means that the energy is condensed on the Doppler shift component.

4.1 Impact of TSE on coherent detection

According to [18], normalized interference power (NIP) is defined to evaluate the statistical impact of TSE, i.e.

$$NIP = \frac{\sum_{l=1}^{M-1} E[A(l)A^*(l)]}{E[A(0)A^*(0)]}, \tag{18}$$

where $E[\cdot]$ denotes statistical expectation of the argument and superscript $*$ is the complex conjugate of the transpose.

In fact, if δt_n is an unknown periodical determinant, substituting eq. (17) into eq. (18), we can express NIP as

$$NIP_d = \frac{\sum_{l=1}^{M-1} |A(l)|^2}{|A(0)|^2} = \frac{1 - |A(0)|^2}{|A(0)|^2}, \tag{19}$$

where subscript d denotes that the sampling instant error is already determined. Then, we have $|A(0)|^2$

$$|A(0)|^2 = \frac{1}{M} + \frac{1}{M^2} \sum_{n=0}^{M-1} \sum_{m=0}^{M-1} \exp(\mathrm{j}2\pi f_d(\delta t_n - \delta t_m)). \tag{20}$$

Let $\Delta = \delta t_{m+1} - \delta t_m$, then eq. (20) can be simplified into

$$|A(0)|^2 = \frac{1}{M} + \frac{1}{M^2} \sum_{n=0}^{M-1} (M - n) \cos(2\pi f_d n \Delta). \tag{21}$$

If $\Delta = 0$, then $|A(0)|^2 = 1$, corresponding to the ideal synchronous sampling case.

In practice, the time-base of non-cooperative radar illuminators, such as weather forecast radar and air traffic control radar adopted for this application, is imperfect, while the time base in passive receiving system is totally independent. Therefore, the stochastic jitter between the PRF and sampling clock cannot be ignored. Then, let

$$\Delta_{nm} = \Delta t_n - \Delta t_m, \tag{22}$$

where Δ_{nm} is considered to be a stochastic variable. Eq. (17) makes sense in this case, representing the relationship between the data sampling sequence and its spectrum. The NIP expressions will be derived when Δ_{nm} is uniform distribution or Gaussian distribution.

If Δ is uniformly distributed in the interval $(-T_s, T_s)$, then its characteristic function will be [19] $\Phi(t) = E[\exp(\mathrm{j}t\Delta)] = \mathrm{sinc}(T_s t)$. Thus, it is easy to calculate $E[|A(0)|^2]$ as follows:

$$E[|A(0)|^2] = \frac{1}{M} + \left(1 - \frac{1}{M}\right) \mathrm{sinc}(2\pi f_d T_s). \tag{23}$$

Substituting eq. (23) into eq. (18), we have

$$NIP_U = \frac{(M-1)[1-\mathrm{sinc}(2\pi f_d T_s)]}{(M-1)\mathrm{sinc}(2\pi f_d T_s)+1}, \tag{24}$$

where the subscript U denotes that Δ_{nm} is uniformly distributed.

If Δ is a zero mean Gaussian variable with variance T_s^2, then its characteristic function is (see [19]) $\Phi(t) = E[\exp(\mathrm{j}t\Delta)] = \exp[-T_s^2 t^2/2]$. Similarly, we have

$$E[|A(0)|^2] = \frac{1}{M} + \left(1-\frac{1}{M}\right)\exp[-2(\pi f_d T_s)^2]. \tag{25}$$

Then,

$$NIP_G = \frac{(M-1)[1-\exp[-2(\pi f_d T_s)^2]}{(M-1)\exp[-2(\pi f_d T_s)^2]+1}, \tag{26}$$

where the subscript G denotes that Δ is Gaussian distribution.

The NIP of these two cases is illustrated in Figure 4 for f_d=5 kHz, $T_s = 10$ μs. Figure 4 shows that the NIP will increase rapidly with respect to the standard variance of Δ. The coherence between pulses will be ruined severely if the standard variance of Δ becomes larger. In this case, the energy leakage will be more and more severe since there are $M-1$ new frequency components caused by TSE.

When the standard variance of Δ deteriorates to a critical value, mathematical values of $\mathrm{sinc}(2\pi f_d \delta t_s)$ and $\exp[-2(\pi f_d\ T_s)^2]$ approximate to zero, and then NIP is almost equal to $M-1$. Since the sampling sequence will no longer remain coherent between pulses, the limited magnitude of $f_d + lr_r/M$ for all l will be zero. However, when the standard variance of Δ approximate to zero, NIP will be approximate to zero in the sense of limitation. In theory, when $f_d T_s$ approximate to zero, the mathematical values of $\mathrm{sinc}(2\pi f_d \delta t_s)$ and $\exp[-2(\pi f_d T_s)^2]$ approximate to unity, such that the values of eqs. (24) and (26) almost have nothing to do with M; thus NIP will be zero. Therefore,

$$0 < NIP < M-1. \tag{27}$$

Observing Figure 4, we may find that the coherence in the pulses will be in a good state if $f_d T_s$ is not that large and M is constant. The NIP will be larger when Δ is uniform distribution, since the uniform distribution is the worst assumption for Δ. In this case, we have no prior knowledge about Δ. While $f_d T_s$ becomes larger, the coherence in the pulses is ruined completely; as a result, no processing gain would be achieved. Thus, the NIP will approximate to a constant in these two assumptions.

In fact, the energy leakage of the signal component will make the noise level rise. The NIP can be considered as SNR loss due to the effect of TSE. Therefore, it is rational to use NIP as a standard to evaluate the performance of coherent integration in passive coherent radar.

4.2 Doppler frequency estimation error caused by TSE

In ideal implementation of data sampling, let the combined in-phase and quadrature components of the first sample for each pulse be $A_s \exp(\mathrm{j}2\pi f_d n T_r)$, where n is the ordinal number of pulses. Applying M samples to DFT analysis, we will have Doppler resolution bins of size $1/MT_r$. For simplicity, the quantization effect will be neglected in the following discussion. Let the input Doppler frequency fall precisely into the center of one Doppler bin, i.e. $f_d = k/(MT_r)$, then, we can express the input samples as $A_s \exp(\mathrm{j}2\pi(k/(MT_r))nT_r)$.

In practice, the actual sample interval between pulses is $T_r' = T_r + \Delta T_r$. Then, the combined in-phase and quadrature components of the first sample for the nth pulse can be expressed as

$$A_s \exp\left(\mathrm{j}2\pi \frac{nk}{MT_r}(T_r+\Delta T_r)\right) = A_s \exp\left(\mathrm{j}2\pi\left(\frac{k}{MT_r}\right)nT_r\left(\frac{T_r+\Delta T_r}{T_r}\right)\right). \tag{28}$$

The estimated Doppler frequency f' of the signal will be

$$f' = f + \Delta f = \frac{k}{MT_r}\frac{T_r+\Delta T_r}{T_r}, \tag{29}$$

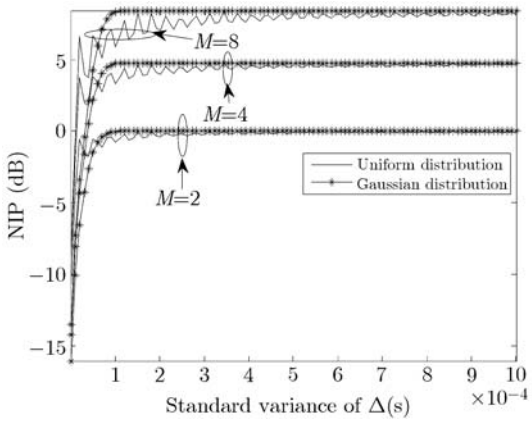

Figure 4 NIP in asychronous sampling.

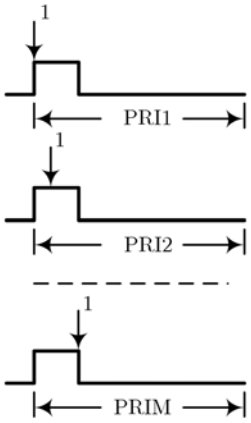

Figure 5 M pulses for coherent integration.

which implies a bias in Doppler measurement. And the Doppler bias is $\Delta f = k\Delta T_r/MT_r^2$. Let the sample drift of the first sample for the M pulses be an entire pulse width T, or sampling interval T_s, as illustrated in Figure 5. Then

$$\Delta T_r = \frac{\min(T, T_s)}{M}. \tag{30}$$

The corresponding Doppler frequency bias is

$$\Delta f = k\frac{\min(T, T_s)}{(MT_r)^2}. \tag{31}$$

In general, according to the Nyquist sampling theorem, we have $T_s < T$, such that

$$\Delta f = \frac{kT_s}{(MT_r)^2} = \frac{1}{(MT_r)}\frac{k}{N}. \tag{32}$$

The first term in eq. (32) is Doppler cell size. If $kT_s << MT_r$, then the second term is small with respect to Doppler cell size. However, if $k = T_r/T_s = N_p$, then the Doppler bias will be

$$\Delta f = \frac{kT_s}{M^2T_r}. \tag{33}$$

Thus, the Doppler bias will depend on the Doppler cell size and the periodicity of relative sampling instant. The Doppler estimation bias due to asynchronous sampling for different integration numbers of pulses is illustrated in Figures 6 and 7, where $PRF = 1000$ and 2200 Hz. From the theoretical analysis and the simulational results, it can be concluded that: 1) If the periodicity of relative sampling instant is a constant, then the Doppler bias will be larger for signals with higher Doppler frequency; 2) Doppler bias is relatively small for larger M, and it can be neglected for the cases illustrated in Figure 6 and Figure 7.

Simulation analysis of Doppler bias for different Doppler frequencies are presented as follows. Let the actual PRF of the signal considered be 1 kHz with duty cycle 0.5, and let the sampling frequency be 40 kHz. Here, Doppler shifts are 400 and 100 Hz, respectively. The results of coherent integration involved in 20 pulses for different N_p are given in Figures 8 and 9, respectively. The periodicity of relative sampling instant is 10 PRIs for $N_p = 40.1$ or $N_p = 40.9$. Even though we have the same size of Doppler cell in the two cases, the Doppler bias is relatively small for $N_p = 40.9$. Since the samples for $N_p = 40.9$ is larger than the other case in number, the sequences contains more information about the actual signal.

Comparing Figure 8 with Figure 9, we find that the Doppler bias will be larger for signals with higher Doppler frequency when the total number of samples N for coherent integration is a constant. In fact, the Doppler cell number k corresponding to the larger input Doppler frequency will be bigger, which in agreement with the conclusion reached from eq. (32).

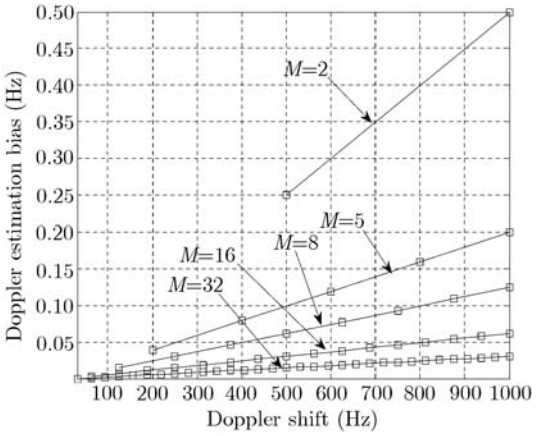

Figure 6 Doppler bias due to asynchronous sampling.

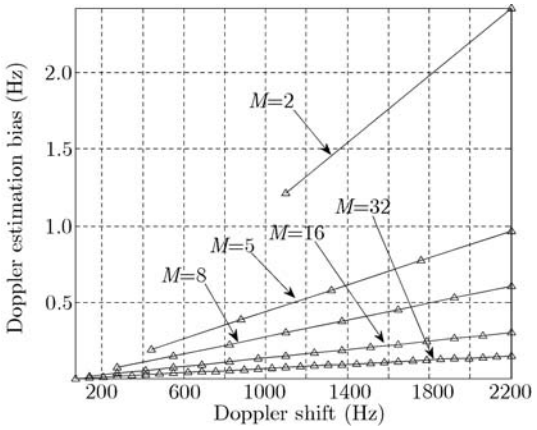

Figure 7 Doppler bias due to asynchronous sampling.

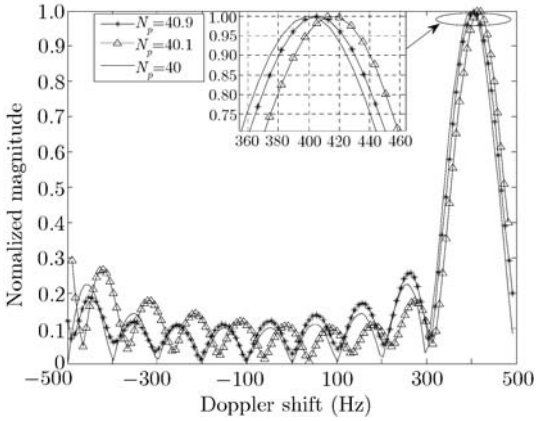

Figure 8 Doppler frequency estimation for f_d=400 Hz, $M = 10$.

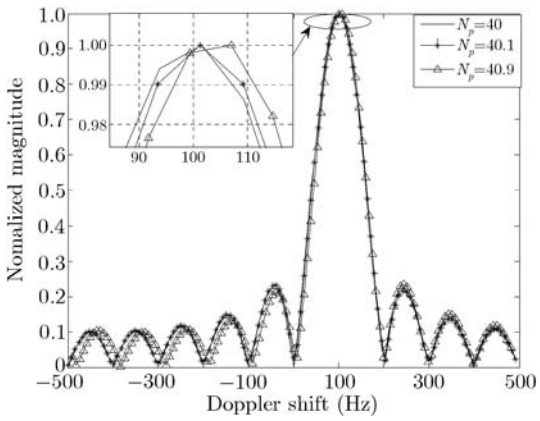

Figure 9 Doppler frequency estimation for f_d=100 Hz, $M = 10$.

5 Conclusions

In this paper, we focused on the impact of time synchronization error. The periodicity of relative sampling instant variation of each pulse was explored via modelling. And the normalized interference power (NIP) was defined to assess the potential impact of the time synchronization error (TSE). The NIP analytical expressions were achieved when the differences between the adjacent relative sampling instant is uniform distribution or Gaussian distribution. At the same time, the Doppler frequency bias expression caused by TSE was obtained. Simulation results in the cases of different periods of relative sample instant variation verified the theoretical analysis in this paper. The main conclusions we achieved in this paper are as follows:

1) By eq. (16), there are $M-1$ new spurious frequency components in the digital spectrum in the case of asynchronous sampling. All these spurious spectral lines are located in the vicinity of Doppler shift component, which may cause false alarm in these range-doppler cells.

2) If the standard variance of the periodicity of relative sampling instant deteriorates to a critical value, the sampled sequence will no longer remain coherent between pulses. Then, the detection performance of passive coherent receiver will decrease.

3) The Doppler bias will be larger for signals with higher Doppler frequency. It is relatively small for large M.

These conclusions will be useful for the analysis of passive coherent detection and parameters estimation.

Acknowledgements

This work was supported by the National Natural Science Foundation of China (Grant Nos. 60672139, 60972160).

References

1 Qi R, Coakley F P, Evans B G. Practical consideration for band-pass sampling. IEE Electr Lett, 1996, 32: 1861–1862
2 Ma B T, Fan H Q, Fu Q. IF sampling conditions for coherent pulse radar (in Chinese). J Data Acquis Process, 2009, 24: 114–118
3 Zhu Y L, Fan H Q, Ma B T, et al. Design of IF signal acquisition system for pulse coherent radars (in Chinese). Syst Eng Electr, 2009, 31: 489–496
4 Wang X M, Kuang Y S, Chen Z X. Surveillance Radar Technology (in Chinese). Beijing: Publishing House of Electronics Industry. 2008. 366–369
5 Thomas D D. Synchronization of noncooperative bistatic radar receivers. PhD Dissertation. Syracuse University, 1999
6 Yang Z Q, Zhang Y S, Luo Y J. Bistatic/Multistatic Radar System (in Chinese). Beijing: Publishing House of National Defense Industry, 1998. 209–214
7 Wang W Q, Ding C B, Liang X D. Time and phase synchronization via direct-path signal for bistatic synthetic aperture radar systems. IET Radar Sonar Navig, 2008, 2: 1–11
8 Jenq Y C. Digital spectra of non-uniformly sampled signals: fundamentals and high-speed waveform digitizers. IEEE Trans Instrum Measur, 1988, 37: 245–251
9 Jenq Y C. Digital spectra of non-uniformly sampled signalsdigital look-up tunable sinusoidal oscillators. IEEE Trans Instrum Measur, 1988, 37: 358–362
10 Tarczynski A, Valimaki V, Cain G D. FIR filtering of non-uniformly sampled signals. In: IEEE Inter Con ASSP, New Paltz, NY, USA, 1997. 2237–2240
11 Jenq Y C. Perfect reconstruction of digital spectrum from non-uniformly sampled signals. In: IEEE Instrumentation and Measurement Technology Conference, Ottawa, Canada, 1997. 19–21
12 Tao W W, Zhang J Q, Lu Q Y. Spectral interpolated compensation analysis of non-coherent sampling signals (in Chinese). J Fudan Univ (Nat Sci), 2008, 47: 703–709
13 Geng X P, Hu Y H, Yan H H, et al. An improved imaging algorithm for fixed-receiver bistatic SAR. Sci China Inf Sci, 2010, 53: 1461–1469
14 Hang L, Jing W, Xing M D, et al. Unparallel trajectory bistatic spotlight SAR imaging. Sci China Ser F-Inf Sci, 2009, 52: 91–99
15 Kulpa K S, Czekala Z. Masking effect and its removal in PCL radar. IEE Radar Sonar Nav, 2005, 152: 174–178
16 Griffiths H D, Baker C J. Passive coherent location radar systems Part 1: performance prediction. IEE Radar Sonar Nav, 2005, 152: 153–159
17 Howland P E, Maksimiuk D, Reitsma G. FM radio based bistatic radar. IEE Radar Sonar Nav, 2005, 152: 107–115
18 Choi Y S, Voltz P J, Casara F A. On channel estimation and detection for multicarrier signals in fast and selective Rayleigh fading channels. IEEE Trans Commun, 2001, 49: 1375–1387
19 Lu D J. Stochastic Process with Application (in Chinese). Beijing: Publishing House of Tsinghua Univ., 2007. 661–662

Appendix

The derivation of eq. (16) are as below.

$$\begin{aligned}
X(f,i) &= \sum_{N=0}^{+\infty} \widetilde{x}(N,i)\exp[-\mathrm{j}2\pi f(NT_r+iT_s)] \\
&= A_s\sum_{k=0}^{+\infty}\sum_{n=0}^{M-1}\widetilde{s}_T(kMT_r+nT_r+\delta t_n+iT_s)\exp[\mathrm{j}2\pi f_d(kMT_r+nT_r+\delta t_n+iT_s)] \\
&\quad\cdot\exp\{-\mathrm{j}2\pi f[(kM+n)T_r+iT_s]\} \\
&= A_s\exp[\mathrm{j}2\pi(f_d-f)iT_s]\sum_{k=0}^{+\infty}\exp[\mathrm{j}2\pi(f_d-f)kMT_r]\sum_{n=0}^{M-1}\widetilde{s}_T(kMT_r+nT_r+\delta t_n+iT_s) \\
&\quad\cdot\exp[\mathrm{j}2\pi(f_d-f)nT_r]\exp(\mathrm{j}2\pi f_d\delta t_n) \\
&= A_s\exp[\mathrm{j}2\pi(f_d-f)iT_s]\sum_{k=0}^{+\infty}\exp[\mathrm{j}2\pi(f_d-f)kMT_r]\sum_{n=0}^{M-1}\frac{1}{2\pi}\int_{-\infty}^{+\infty}S(\Omega)\exp[\mathrm{j}\Omega((kM+n)T_r+iT_s)]d\Omega
\end{aligned}$$

$$
\begin{aligned}
&\cdot \exp(\mathrm{j}2\pi(f_d - f)nT_r)\exp(\mathrm{j}2\pi f_d \delta t_n)\\
&= A_s \exp[\mathrm{j}2\pi(f_d - f)iT_s]\sum_{n=0}^{M-1}\exp(\mathrm{j}2\pi f_d\delta t_n)\frac{1}{2\pi}\int_{-\infty}^{+\infty}S(\Omega)\Big\{\sum_{k=0}^{+\infty}\exp[\mathrm{j}(\Omega + 2\pi(f_d - f))kMT_r]\Big\}\\
&\quad \cdot \exp[\mathrm{j}(\Omega + 2\pi(f_d - f))nT_r + iT_s)]d\Omega\\
&= A_s \exp[\mathrm{j}2\pi(f_d - f)iT_s]\sum_{l=-\infty}^{+\infty}\sum_{n=0}^{M-1}\exp(\mathrm{j}2\pi f_d\delta t_n)\frac{1}{MT_r}\int_{-\infty}^{+\infty}S(\Omega)\delta\Big[\Omega + 2\pi(f_d - f) - \frac{2\pi l}{MT_r}\Big]\\
&\quad \cdot \exp[\mathrm{j}(\Omega + 2\pi(f_d - f))nT_r]\exp[\mathrm{j}\Omega(iT_s)]d\Omega\\
&= A_s \exp[\mathrm{j}2\pi(f_d - f)iT_s]\frac{1}{MT_r}\sum_{n=0}^{M-1}\exp(\mathrm{j}2\pi f_d\delta t_n)\sum_{l=-\infty}^{+\infty}S\Big(2\pi f - 2\pi f_d - \frac{2\pi l}{MT_r}\Big)\\
&\quad \cdot \exp\Big(-\mathrm{j}\frac{2\pi ln}{MT_r}\Big)\exp\Big[-\mathrm{j}2\pi\Big(f_d - f + \frac{l}{MT_r}\Big)iT_s\Big]\\
&= A_s\frac{1}{T_r}\sum_{l=-\infty}^{+\infty}\Big\{\sum_{n=0}^{M-1}\exp(\mathrm{j}2\pi f_d\delta t_n)\exp\Big(-\mathrm{j}\frac{2\pi ln}{M}\Big)\Big\}\exp\Big[\mathrm{j}2\pi\Big(-\frac{l}{MT_r}\Big)iT_s\Big]S\Big(2\pi f - 2\pi f_d - \frac{2\pi l}{MT_r}\Big)\\
&= A_s\frac{1}{T_r}\sum_{l=-\infty}^{+\infty}S\Big(2\pi f - 2\pi f_d - \frac{2\pi l}{MT_r}\Big)\exp\Big[\mathrm{j}2\pi\Big(-\frac{l}{MT_r}\Big)iT_s\Big].
\end{aligned}
$$